Ni-NHC Nanoparticles in Micelles as an Effective and Reusable Catalyst for Hydrogenations and Reductive-Aminations in Water

Marta G Avello, Jorge Blas Martínez, Thierry Romero, Vasiliki Papaefthimiou, Michael J Chetcuti, Vincent Ritleng, Cuong Pham-Huu, Claude Oelschlaeger, Christophe Michon

Ni-NHC Nanoparticles in Micelles as an Effective and Reusable Catalyst for Hydrogenations and Reductive-Aminations in Water

Marta G. Avello,[†,#] Jorge Blas Martínez,[†] Thierry Romero,[‡] Vasiliki Papaefthimiou,[‡] Michael J. Chetcuti,[†] Vincent Ritleng,[†] Cuong Pham-Huu,[‡,#] Claude Oelschlaeger,[,§] Christophe Michon*[,†,#]*

[†] Université de Strasbourg, Université de Haute-Alsace, Ecole européenne de Chimie, Polymères et Matériaux, CNRS, LIMA, UMR 7042, 25 rue Becquerel, 67087 Strasbourg, France.

[#] Institut des Etudes Avancées de l'Université de Strasbourg (USIAS), 5 allée du Général Rouvillois, 67083 Strasbourg, France

[‡] Université de Strasbourg, Ecole européenne de Chimie, Polymères et Matériaux, CNRS, ICPEES, UMR 7515, 25 rue Becquerel, 67087 Strasbourg, France.

[§] Karlsruher Institut für Technologie (KIT), Institut für Mechanische Verfahrenstechnik und Mechanik Bereich: Angewandte Mechanik, Gotthard-Franz-Str. 3, Geb. 50.31 Raum 206, 76131 Karlsruhe, Germany

KEYWORDS

Nickel, N-Heterocyclic Carbene ligand, Nanocatalysis, Micelles, Hydrogenation, Reductive amination

ABSTRACT

Nickel metallomicelles were formed through the self-assembly of NHC-olefin-coordinated nickel nanoparticles and sodium dodecyl sulfate (SDS) as a surfactant in water. The reduction of various organic compounds was catalyzed using hydrogen gas within water and without any organic cosolvent. The resulting nickel nanoparticles coordinated to NHC-olefin ligands and coated by a bilayer SDS surfactant structure proved to be effective, selective and reusable catalysts for the hydrogenations of alkenes, alkynes and nitroarenes, as well as for the reductive-aminations of aldehydes with primary amines. The hydrogenations were scaled up to 6 mmol and the catalyst was recycled over 10 runs without any significant loss of activity.

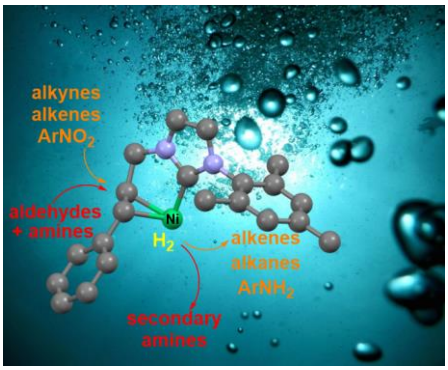

INTRODUCTION

The quest for effective and sustainable chemical reactions has led to the confinement of various catalysts in porous solids, hollow materials and self-assembled structures. If the recycling of the catalytic species is often the desired achievement, such confinement strategies have resulted in other significant benefits such as the stabilization of the catalytic species, higher reactivities, enhanced reaction selectivities and activities due to the reduction of reaction entropies.[1,2] Metal nanoparticles (NPs) are one of the privileged species that have been confined. Among the different explored strategies,[1] the combination of metal NPs and surfactants has resulted in metallomicelles through appropriate design and cooperative self-assembly.[3-10] An interesting approach to prevent agglomeration of the metal NPs has implied the formation of a bilayer assembly of surfactants on the NP surface.[11-15] An outer layer defines the hydrophobic domains, and an inner layer interacts with the NPs, both surfactant layers being connected through hydrophobic interactions. Catalytic applications of metallomicelles appear promising for the sustainable synthesis of bulk and fine chemicals and for catalyst recycling. For example, several systems based on Pd/C, Pd organometallics or nanoparticles have been reported as effective catalysts for cross-coupling reactions,[5,16-18] transfer hydrogenations[5,19-25] and hydrogenations.[26-32] Indeed, such metallomicelles have hydrophobic / lipophilic inner cores that allow the solubilization of organic reagents as well as the catalysis of their reactions, and hydrophilic exterior domains. The catalytic processes within their inner core can proceed in water and a full separation of the organic products from the aqueous reaction medium is possible through extraction, decantation or filtration. In spite of these significant advances for sustainable chemical reactions, small amounts of organic solvents are often required to help in solubilizing the organic reagents or the catalyst in the micelles. However, the use of organic solvents

represents a large source of waste in the chemical production and is also responsible for the major impact on climate change as analyzed recently by Lipshutz and coworkers.[33] Therefore, chemical reactions performed in water without the use of any other solvent are highly desirable.

The major issues in the application of metal NPs in catalysis are their agglomeration and their subsequent deactivation. In order to prevent such drawbacks and simultaneously direct NP properties, different metal-support interactions[1] and/or the use of organic ligands[34-37] have been investigated. In this context, N-heterocyclic carbenes (NHC), which are now privileged ligands in organometallic chemistry and homogeneous catalysis, have been established as valuable stabilization agents for NPs of precious transition metals.[38-40] However, this strategy is still at its infancy considering the earth-abundant transition metals which have been less applied in catalysis and which have become a priority for economical reasons that are not necessarily valid considering climate change and environment.[33] Thus, to the best of our knowledge, there are only five reports on the use of NHC ligands to stabilize Ni NPs and catalyze chemical reactions, such as Kumada couplings, carbonyl hydrosilylations and alkyne semi-hydrogenation.[41-45] In particular, we have recently reported Ni nanoparticles coordinated to NHC ligands bearing an N-coordinated cinnamyl moiety that are readily prepared by the reduction of a [NiCpBr(NHC-cinnamyl)] complex with methyl magnesium bromide and that catalyze effectively the (*Z*)-selective semi-hydrogenation of alkynes and ynamides (Scheme 1).[45] Following these first achievements, we now report the confinement of Ni-NHC-olefin nanoparticles in micelles and further applications of the resulting self-assembled structures in water as effective and reusable catalyst for solvent-free hydrogenations of alkenes, alkynes and nitroarenes and reductive-aminations of aldehydes with amines.

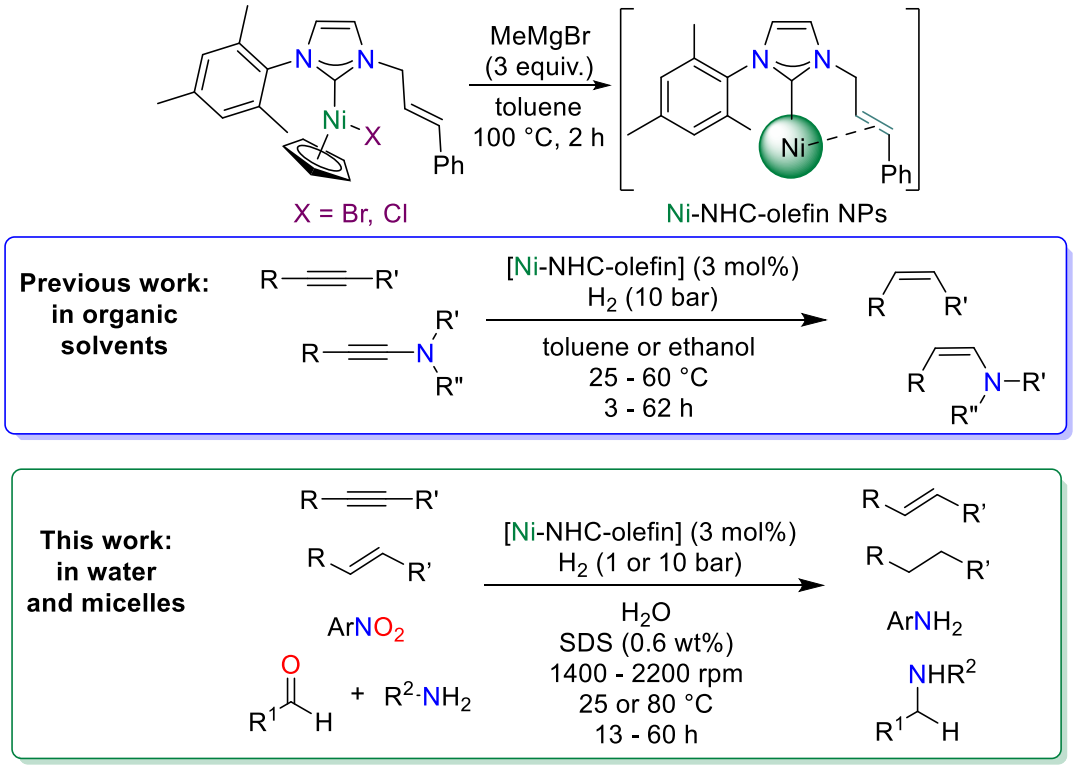

Scheme 1. Previous and present work in catalyzed hydrogenations using Ni-NHC-olefin NPs.

EXPERIMENTAL SECTION

Pre-catalyst synthesis and NHC-olefin-Ni nanoparticles preparation

A Schlenk tube containing a stirring bar was loaded with 3-cinnamyl-1-mesityl-1*H*-imidazolium chloride (500 mg, 1.47 mmol, 1.0 equiv.) and nickelocene (323 mg, 1.47 mmol, 1.0 equiv.) under Ar. The mixture was stirred under Ar in refluxing THF (22 mL) for 48 h until the solution color changed to burgundy. The resulting mixture was filtered through a Celite pad and washed with THF (3 x 10 mL). After solvent evaporation under vacuum, the resulting residue was washed with pentane (3 x 10 mL) under Ar to afford the pure complex – pre-catalyst **1** as a pink powder (624 mg, 1.35 mmol, 92% yield). Afterward, a Schlenk tube containing a stirring bar was loaded with the nickel pre-catalyst **1** (6.9 mg, 0.015 mmol, 3 mol%), dry toluene (1 mL) and a

1.0-1.5 M solution of MeMgBr in THF (45 µL, 0.045 mmol, 9 mol%) under Ar. The resulting solution was stirred at 100 °C for 2 h during which a change of color was observed, from pink to dark brown. The solvent was then evaporated under vacuum to yield a dark gray solid.

General procedure for the catalytic hydrogenations

A Schlenk tube containing a stirring bar and the previously generated NHC-olefin-Ni nanoparticles was loaded with a surfactant: SDS [29 mg, 0.1 mmol (0.6 wt%, 0.02 M)] or Brij35 [30 mg, 0.025 mmol (0.6 wt%, 0.005 M)]. The resulting mixture was dried under vacuum for 10 min. and the organic substrate (0.5 mmol, 1.0 equiv.) was added under Ar. This was followed by the addition of 5 mL of degassed ultrapure water (resistivity 18.2 MΩ.cm at 25 °C and conductivity 0.056 µS/cm at 25 °C). The mixture contained in the Schlenk tube was then placed in an ultrasonic bath (37 kHz, 80 W power) until it looked homogeneous, and subsequently transferred under Ar to an autoclave that was previously dried under vacuum for 1 h. The reactor was loaded with 1 or 10 bar of H_2 and placed under a vigorous stirring (1400 rpm) in a bath at the desired reaction temperature during the whole reaction (13 to 62 h). After stopping the reaction, the reactor was cooled to room temperature and the hydrogen gas was released. An extraction of the reaction mixture was carried out with CH_2Cl_2 or Et_2O (3 x 5 mL). After drying with $MgSO_4$, the organic extract was filtered through a pipette loaded with cotton and silica (2 cm height) followed by a wash with more solvent. The conversion was determined by GC or ^1H NMR spectroscopy, and the product was purified by preparative TLC (previously treated with 5% NEt_3 in the case of nitro derivatives) or Kugelrohr distillation.

General procedure for the reductive amination reactions.

A Schlenk tube containing a stirring bar and the previously generated NHC-olefin-Ni nanoparticles was loaded with SDS surfactant [29 mg, 0.1 mmol (0.6 wt%, 0.02 M)]. The resulting mixture was dried under vacuum for 10 min. and the aldehyde (0.5 mmol) and amine (0.5 mmol) were added under Ar. This was followed by the addition of 5 mL of degassed ultrapure water (resistivity 18.2 MΩ.cm at 25 °C and conductivity 0.056 µS/cm at 25 °C). The mixture contained in the Schlenk tube was then placed in an ultrasonic bath (37 kHz, 80 W power) until it looked homogeneous, and subsequently stirred at 1400 rpm and 80°C for 2 to 12 h. After this time, the reaction medium was transferred under Ar to an autoclave that was previously dried under vacuum for 1 hour. The reactor was loaded with 10 bar of H_2 and placed under vigorous stirring (1400 rpm) in a bath at 80 °C for 48 h. After stopping the reaction, the reactor was cooled to room temperature and the hydrogen gas was released. An extraction of the reaction mixture was carried out with CH_2Cl_2 or Et_2O (2 x 5 mL). After drying with $MgSO_4$, the organic extract was filtered through a pipet loaded with cotton and silica (2 cm height) followed by a wash with more solvent. The conversion was determined by ^{1}H NMR spectroscopy, and the product was purified by preparative TLC (98:2 to 95:5 of petroleum ether : NEt_3, previously treated with the same mixture) or Kugelrohr distillation.

General Procedure for the catalyst recycling

A Schlenk tube containing a stirring bar and the previously generated NHC-olefin-Ni nanoparticles was loaded with SDS surfactant [29 mg, 0.1 mmol (0.6 wt%, 0.02M)]. The resulting mixture was dried under vacuum for 10 min, and 4-phenyl-1-butyne **2b** (70 µL, 0.5 mmol, 1.0 equiv.) was added under Ar. This was followed by the addition of 5 mL of degassed

ultrapure water (resistivity 18.2 MΩ.cm and conductivity 0.056 µS/cm at 25 °C). The mixture contained in the Schlenk tube was then placed in an ultrasonic bath (37 kHz, 80 W power) until it looked homogeneous, and subsequently transferred under Ar to an autoclave, that was previously dried under vacuum for 1 h. The reactor was loaded with 10 bar of H_2 and placed under vigorous stirring (1400 rpm) in a bath at 35 °C for 13 h. After stopping the reaction, the reactor was cooled to room temperature and the hydrogen gas was released. An addition of CH_2Cl_2 or Et_2O (argon degassed, 5 mL) allowed us to transfer the reaction mixture to a Schlenk tube and then into a 15 mL centrifugation tube. After centrifugation of the mixture at 3000 rpm for 5 min, the organic phase was collected from the bottom of the tubes with a syringe and a needle. Afterward, additional CH_2Cl_2 (or Et_2O, 5 mL) was then added to the aqueous phase for a novel centrifugation procedure for 5 min at 3000 rpm. Afterward, all the collected organic phases were dried over $MgSO_4$ before analyzing the conversion by GC. The aqueous phase was then transferred back to the Schlenk tube and the remaining traces of CH_2Cl_2 or Et_2O were eliminated by evaporation under a moderate vacuum (due to foaming, a gradual degassing / evaporation is required over 15 min until a 30 mbar vacuum). Afterward, 4-phenyl-1-butyne substrate (70 µL, 0.5 mmol, 1.0 equiv.) was added to the aqueous solution contained in the Schlenk tube under Ar and the resulting mixture was placed in an ultrasonic bath (37 kHz, 80 W power) until it looked homogeneous. After the subsequent transfer under Ar of the reaction medium to the autoclave that was previously dried under vacuum for 1 hour, the reactor was loaded with 10 bar of H_2 and placed under vigorous stirring (1400 rpm) in a bath at 35 °C during 13 h to start a new catalytic cycle under similar conditions than those described above.

Caution! After the first cycle (<u>but not the others</u>), 150 mg of NaCl were added to the reaction mixture in order to facilitate the separation of organic and aqueous phase. Furthermore, after

each cycle, 0.5 mL of degassed water was used to help the transfer of the reaction mixture and counterbalance the technical losses. **Caution!** Keeping the same concentration of the catalytic solution and removing cautiously all CH_2Cl_2 or Et_2O traces (due to foaming, a gradual degassing / evaporation is required over 15 min under vacuum until 30 mbar) are crucial for the success of the next catalytic reaction / cycle (see Figure S14).

RESULTS AND DISCUSSION

Catalyst Preparation and Characterization

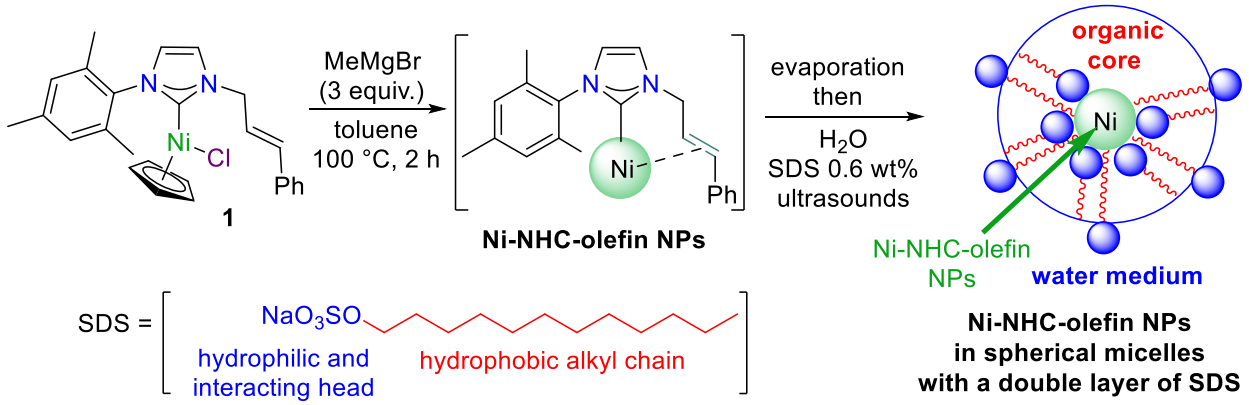

Scheme 2. Synthesis of Ni-NHC-olefin NPs stabilized in micelles with a double layer of SDS.

Based on our previous work,[45] the nickel precatalyst **1** was first reduced using 3 equivalents of MeMgBr in toluene at 100 °C for 2 h (Scheme 2). The reaction mixture whose color changed from pink to dark brown, was then cooled to room temperature and evaporated under vacuum to result in a dark gray solid. The latter was subsequently dissolved in degassed ultrapure water containing 0.6 wt% of sodium dodecyl sulfate (SDS) with the help of ultrasounds to yield an aqueous solution of Ni-NHC-olefin NPs stabilized in micelles (Scheme 2). According to a previous report on Pd NPs stabilized by a zwitterionic surfactant bearing a sulfonate moiety,[15]

the present Ni-NHC-olefin NPs are expected to be coated by a double layer of SDS surfactant, an outer layer defining the hydrophobic domains, i.e. the micelles, and an inner layer interacting with the NPs.

It should be noted here, that prior to the validation of this synthetic procedure, several surfactants were screened and it was found that the use of SDS at 0.6 wt% afforded the best results for the semi-hydrogenation of phenylpropyne **2d** under 1 bar H_2 and 80 °C (Table S1). Surprisingly, a change of the SDS concentration from 0.6 wt% to 0.5 or 0.7 wt% resulted in much less effective catalytic hydrogenations. Such an observation was also noted for Brij 35 and SPGS-550-M (Nok). In addition, according to a screening of the catalyst loading (Table S2), 3 mol% of **1** were required to fully hydrogenate 4-phenyl-1-butyne **2b** and phenylpropyne **2d** under 10 bar H_2, as lower loadings mainly resulted in semi-hydrogenation products with alkene isomers **3b**/**4b** and **3d**/**4d** along with various amounts of alkanes **5b** and **5d**.

XPS analysis of Ni-NHC-olefin NPs in SDS micelles was performed on a sample prepared in a glovebox by drying several drops of the NPs in aqueous solution on a gold surface. The survey scan spectrum revealed the core levels of all expected elements and allowed estimating their surface atomic ratios (Figures 1a, S1, Table S5). However, due to the presence of the SDS surfactant, the Ni 2p core region required a long acquisition time (5 h) to allow the observation of a weak peak of Ni $2p_{3/2}$ at ca. 853.3 eV, without any observable satellite (Figure 1b). Though the binding energy (BE) can be affected by the small size of the particles, the shape of the peak and the unknown position of the satellites do not help to conclude accurately on the oxidation state, this value suggests the presence of a mixture of Ni(0) and Ni(II) species as the BE is in between the metallic (Figure 1d) and oxidized Ni as nanoparticles or element (Figures 1e and 1f) values. By comparison, a stronger peak of Ni $2p_{3/2}$ at ca. 852.5 eV is observed for the

spent catalyst with some traces of Ni(II) due to superficial oxidation during the analytical sample handling. This suggested a complete reduction to Ni(0) during the catalytic hydrogenation (Figure 1c).

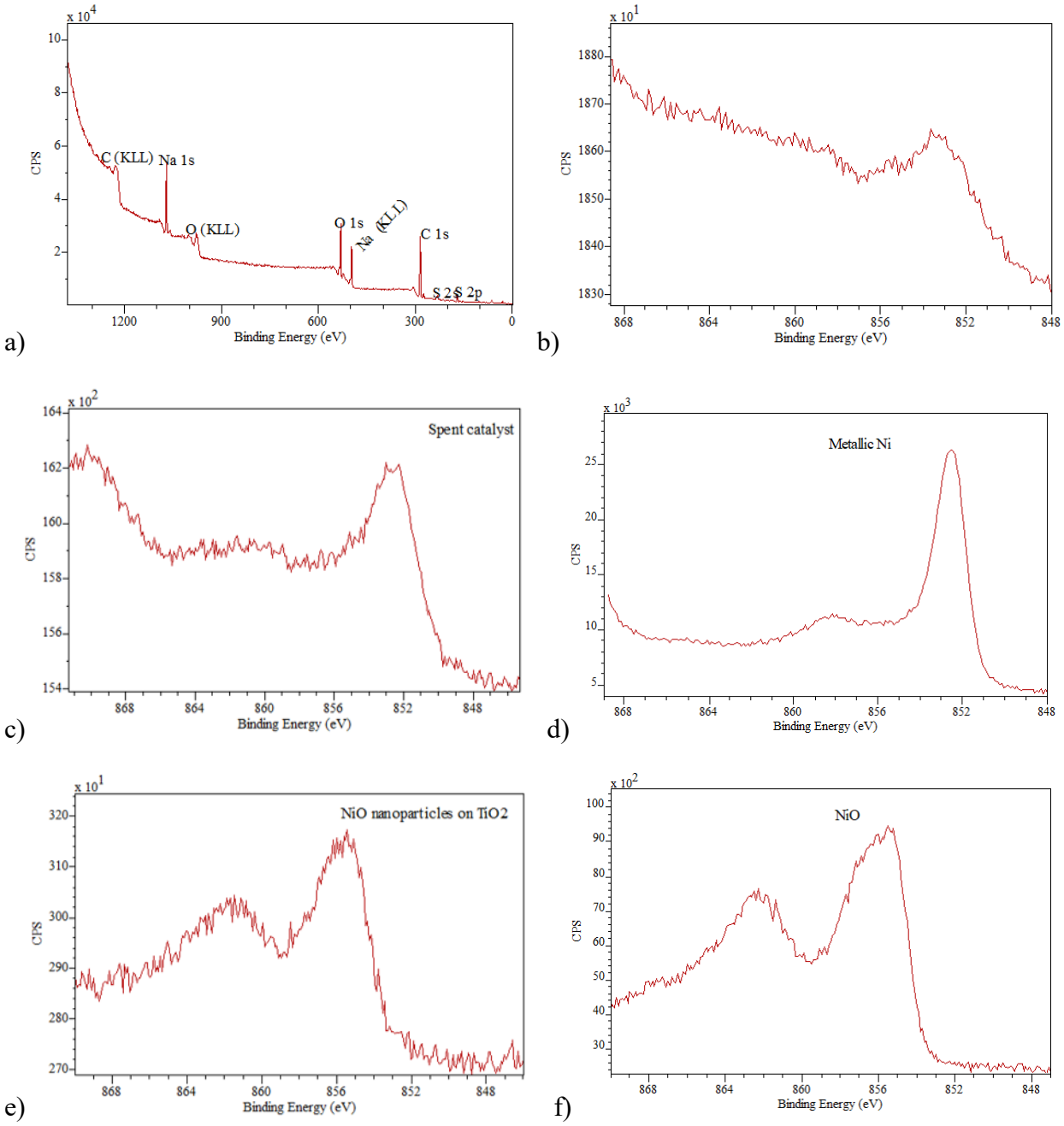

Figure 1. a) XPS survey scan spectrum of Ni-NHC-olefin NPs in SDS-based micelles. Mg (KLL) around 300 ev; b)-f) XPS spectra of Ni $2p_{3/2}$ peaks: b) Ni-NHC-olefin NPs in SDS micelles before catalysis; c) Ni-NHC-olefin NPs in SDS micelles after catalysis, spent catalyst; d) Ni(0); e) Ni(II) of NiO nanoparticles on TiO_2; f) Ni(II) of NiO.

Regarding the XPS spectra of the fresh and spent catalyst, it must be underlined that superficial oxidation can explain the presence of Ni(II) as a nanometer oxidized layer placed on the surface of the Ni(0) catalyst. Despite the precaution taken during the sample transfer before analysis, it is very challenging to avoid such superficial oxidation, or passivation phenomenon.

Cryo-TEM analysis highlighted the formation of spherical micelles of ca 4 - 8 nm in size (black dots in the Figure 2a) together with vesicles of spherical shape from 50 to 1909 nm (Figures 2a-d and S2-S5) and of crystalline aggregates of Ni particles with irregular shapes (Figures 2c-d and S6). It is likely that these spherical micelles and vesicles and other possible species like aggregates of Ni particles covered with monolayers of SDS surfactant[46-52] act as nano- and microreactors for the catalytic hydrogenations of the present study. The presence of vesicles was confirmed by SEM-STEM analysis but further STEM-EDS analysis was not possible due to the vesicles and micelles elusive behavior under vacuum when not frozen (Figure S7). Refereeing on the concept of molecular packing parameter introduced by Israelachvili et al.,[46] the formation of vesicles using only SDS surfactant is not expected. However, according to several studies,[47-49] SDS vesicles can form spontaneously upon addition of various chemicals, as it is the case here with the presence of Ni NPs in solution. By comparison, DLS analysis of a similar sample at a 0.2 mM concentration detected two sets of species, vesicles or aggregates of Ni particles, a major of 247 nm and a minor of 1737 nm, without the spherical micelles of 4-8 nm, as observed by Cryo-TEM (Figure S8).

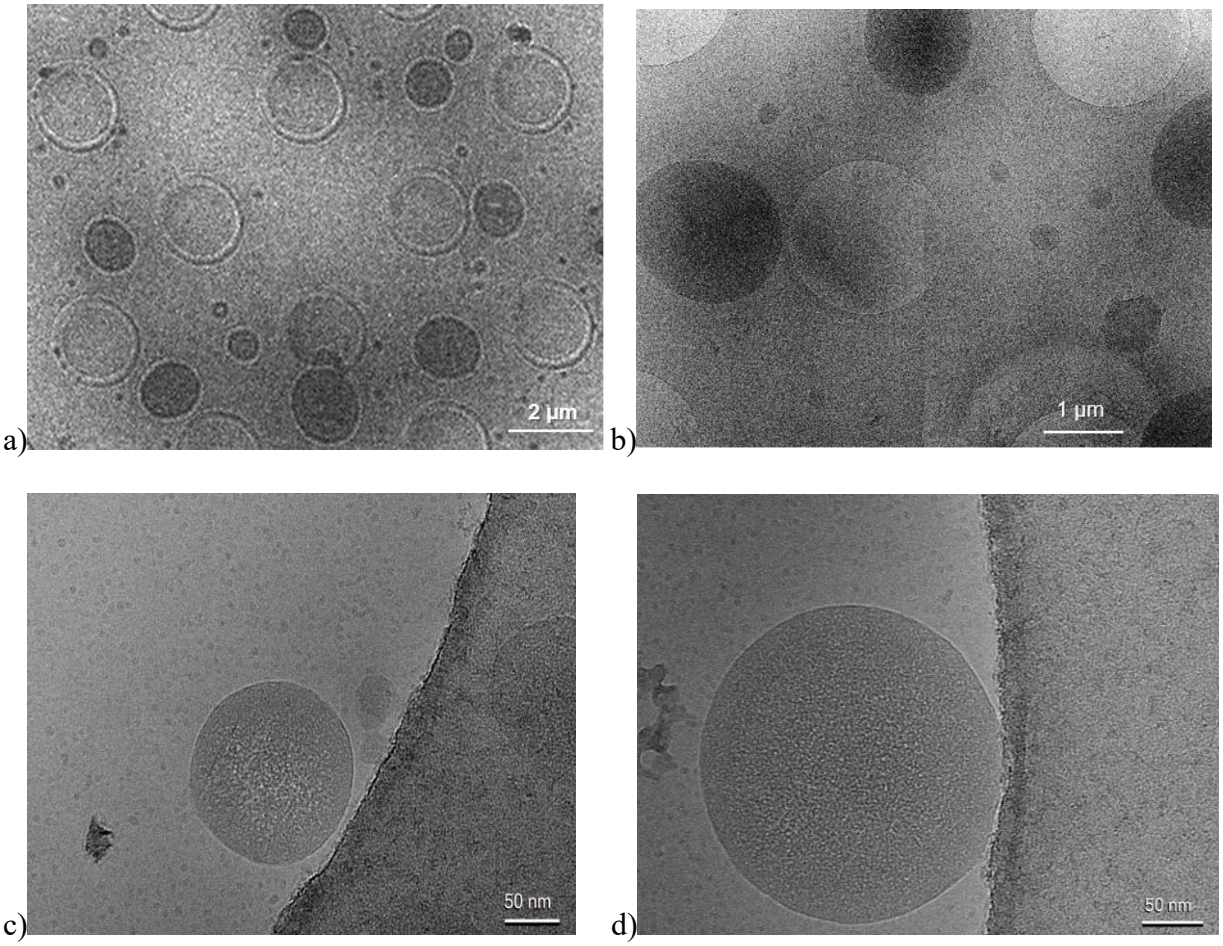

Figure 2. Cryo-TEM analysis of Ni-NHC-olefin NPs in SDS-based micelles.

Analyses by thermogravimetry (TGA and DTGA) confirmed the bilayer SDS surfactant structure coating the Ni NPs by showing a curve with three weight losses (i.e., 120 - 235 °C, 36%; 235 – 670 °C, 12%; and 670 – 900 °C, 6%) (Figure 3). Such a complex weight loss profile is characteristic of bilayer-coated NPs and similar to those reported for water-dispersible nanostructures stabilized by surfactants.[11-15] According to the latter, the decomposition mechanism proceeds by a first weight loss (120 – 235 °C) related to the desorption of the secondary outer layer of SDS together with uncoordinated surfactant (Scheme 2). The following weight loss (235 – 670 °C) likely corresponds to the decomposition of the inner layer of SDS surfactant coordinated to the Ni-NHC-olefin NPs (Scheme 2).

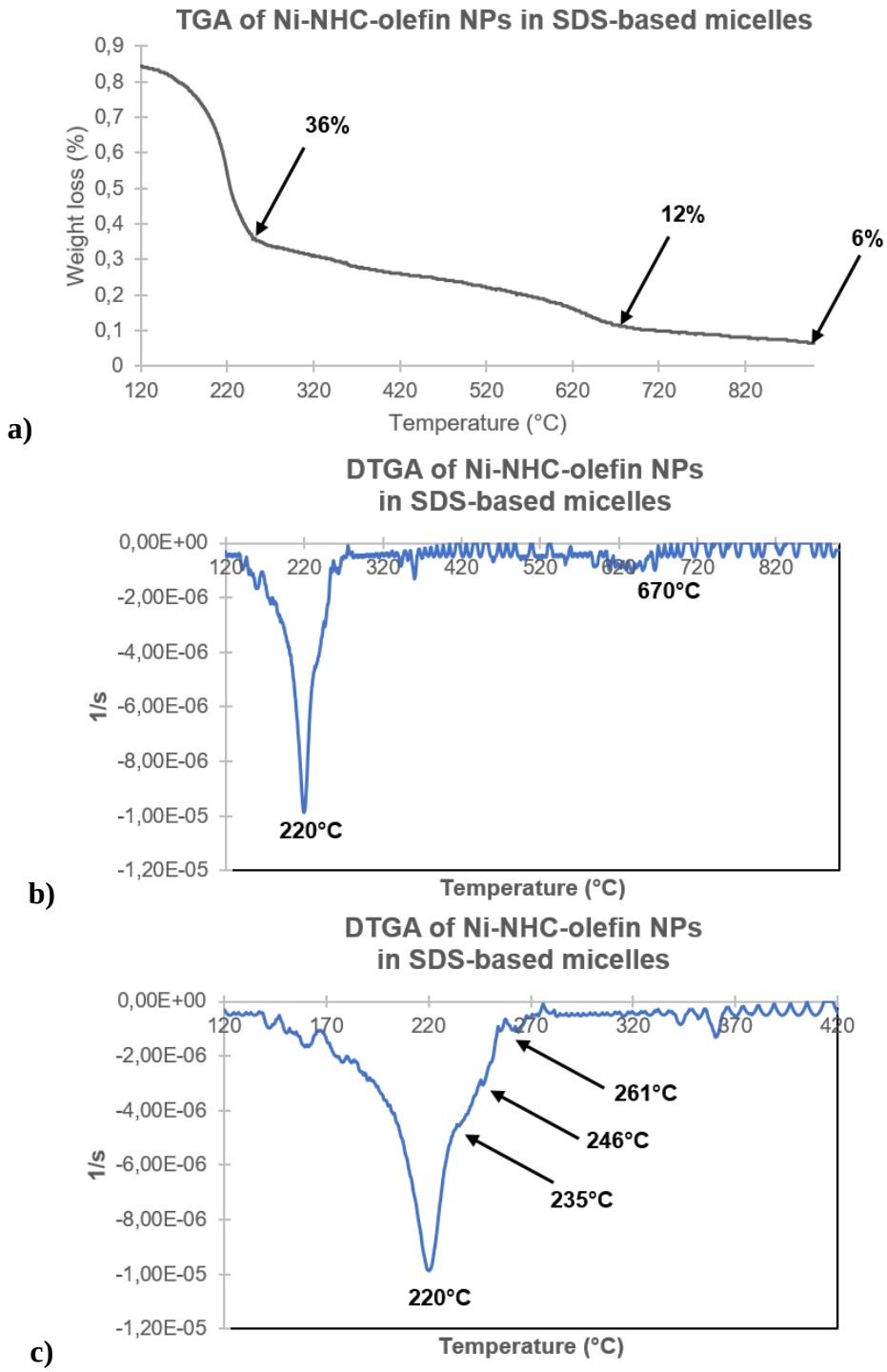

Figure 3. a) Thermogravimetric profile (TGA) of Ni-NHC-olefin NPs (0.015 mmol) in H_2O (5 mL) and SDS (0.6 wt%) based micelles; b), c) derivative of the weight loss per second versus temperature (DTGA).

Solutions of Ni-NHC-olefin NPs in SDS micelles were also analyzed by macro- and microrheology (Figures 3 and S8-S11). The macro-rheology measurements were performed on

aqueous solutions containing either the surfactant SDS (Figures 3a-b), either Brij35 which was used in the surfactant screening (Table S1, Figures 3e-f), with and without phenylpropyne **2d**, in order to compare results with ionic and neutral surfactants and check the effect of an organic chemical on the viscosities. A Newtonian behavior was observed with an almost independent variation of the viscosity as a function of the shear rate with a constant viscosity value close to that of pure water, namely η_{Bulk}=1.2±0.3 mPa.s. Local viscosity values with η_{MPT}=1.5±0.02 mPa.s determined by using multiple particle tracking (MPT) based microrheology are in relatively good agreement with those determined macroscopically (Figures S8 and S9). In all cases, whether in the presence of SDS or Brij35, these low viscosity values are compatible with the formation of spherical micelles. In addition, the statistical analysis of the MSD distribution clearly reveals a homogeneous structure in both cases with a non-Gaussian parameter α close to zero. Moreover, for the system containing SDS spherical micelles, optical microscopy images also confirm the presence of few vesicles of size > 1 µm, as shown in Figure 3c for an alkyne-free aqueous solution. This above system was also investigated by adding 3 M NaCl in order to see how an increase in the ionic strength could induce the formation of SDS elongated "wormlike" micelles[53-55] and how such a change in structure from spherical to elongated micelles could impact the catalytic performances of the metallomicelles.[56-58] As shown in Figures 3d and S10, the addition of 3 M NaCl resulted in a significant number of large aggregates composed of NPs and adsorbed tracer particles of size > 10 µm, preventing any local viscosity measurement using MPT and significantly limiting catalyst activity (Table S3). For solutions with NPs and the surfactant Brij35 in presence of 3 M NaCl, fewer aggregates are formed than with SDS, and no significant changes in viscosity and morphology were observed compared to salt-free solutions (Figure S11).

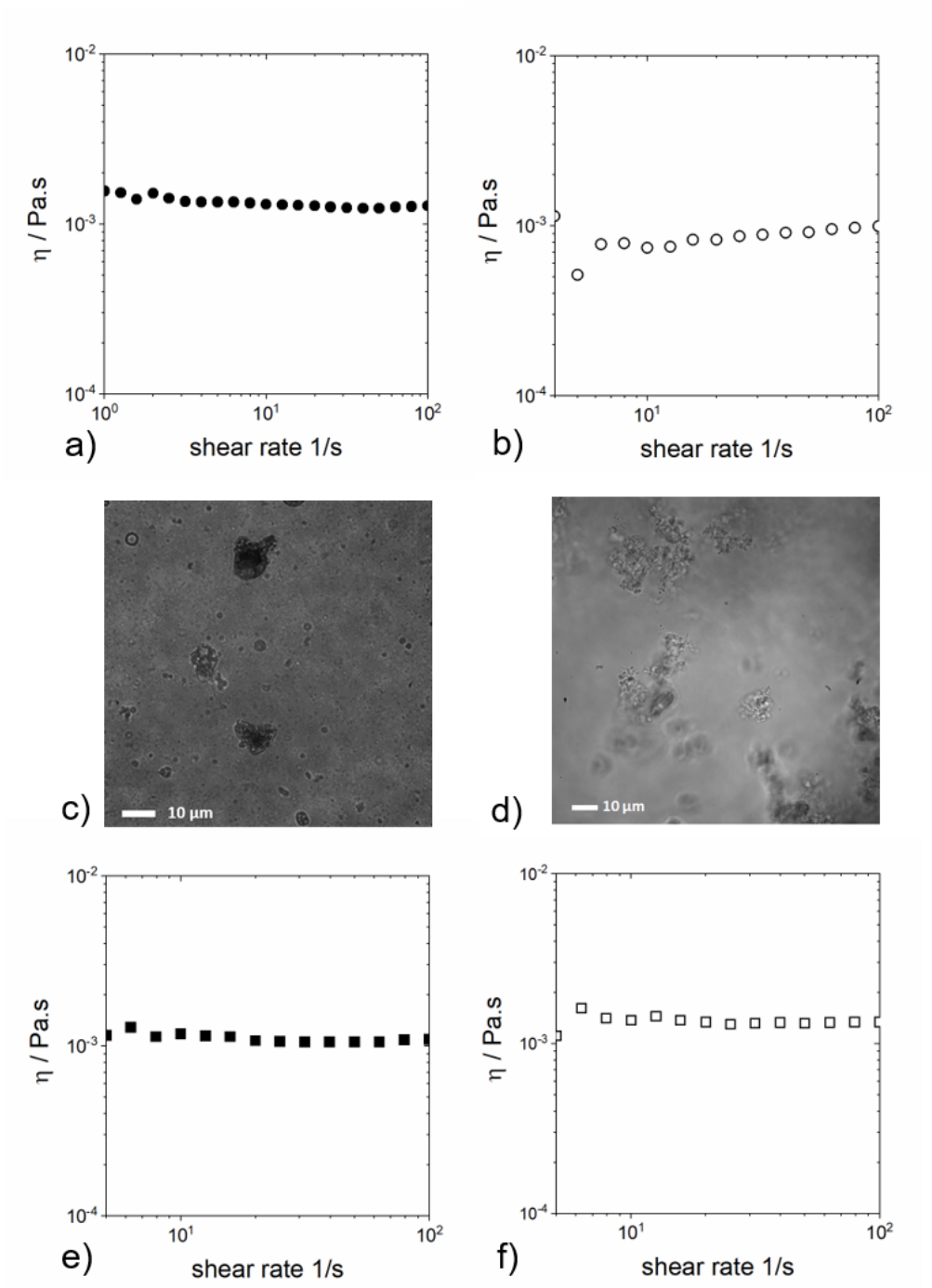

Figure 4. a-b) Rheology measurements of: a) aqueous solution of SDS (0.6 wt%) with [Ni-NHC-olefin] (3 mol%); b) aqueous solution of SDS (0.6 wt%) with [Ni-NHC-olefin] (3 mol%) and alkyne **2d** (0.5 mmol); c-d) optical microscope pictures during microrheology measurements (with PS 0.5 µm) of an aqueous solution of SDS (0.6 wt%) with [Ni-NHC-olefin] (3 mol%) under white light without (c) and with (d) NaCl (3M). e-f) Rheology measurements of: e) aqueous solution of Brij35 (0.6 wt%) with [Ni-NHC-olefin] (3 mol%); f) aqueous solution of Brij35 (0.6 wt%) with [Ni-NHC-olefin] (3 mol%) with alkyne **2d** (0.5 mmol).

Catalytic Activity

Hydrogenation of Alkynes

The catalytic activity of the Ni-NHC-olefin NPs in SDS-based micelles was first studied for the semi- and full hydrogenation of alkynes (Table 1). Terminal alkynes **2a-c** required 10 bar H_2 and 13 h of reaction at room temperature to be reduced to the corresponding alkanes **5a-c** (entries 2-4). Though hydrogenation of **2a** at 1 bar H_2, at 80 °C for 62 h did not proceed (entry 1), internal alkynes **2d-f** were semi-hydrogenated to the corresponding alkenes **3d-f** and **4d-f** in low to excellent yields under the same experimental conditions, leading almost exclusively to the (*E)*-isomers **4d-f** (entries 5,7,9). To the best of our knowledge, this is only the third report of nickel catalyzed (*E*)-selective semi-hydrogenation of alkynes at mild temperatures and low H_2 pressures.[59,60] Under a pressure of 10 bar H_2 for 13 h of reaction at 30 °C, the alkynes **2d-f** were fully hydrogenated to the corresponding alkanes **5d-f** with yields ranging 60% to quantitative (entries 6, 8, 10). By comparison with **2d**, the alkynes **2e** and to some extend **2f** were harder to reduce and led also to various amounts of the corresponding alkenes. Regarding substrate **2f**, the catalytic hydrogenation proceeded well in pure water at 10 bar H_2 for 13 h of reaction at 30 °C but (*Z*)-alkene **3f** was the main product (entry 11). Therefore, surfactant sulfate moieties likely interacted with the substrates to promote and direct the hydrogenation reactions. Within similar conditions, the use of Raney Ni as a catalyst in pure water resulted in the full hydrogenation of **2f** into alkane **5f** (entry 12). Finally, though the alkyne **2g** was selectively semi-hydrogenated to the (*E*)-alkene **4g** in quantitative yields under 1 bar H_2 and 80°C (entry 13), its full hydrogenation did not occur under 10 bar and 30 °C and **4g** was the single hydrogenated product within these conditions (entry 14). By comparison with previous studies on Pd catalysts stabilized by surfactants using 1 or 14 bar H_2 pressure[21,25,28] or hydrogen transfer,[21] our catalytic system was

slower but (*E*)-selective for semi-hydrogenations, Pd catalysts offering (*Z*)-alkenes or alkanes within an hour or less at 25 °C.

Table 1. Catalytic semi- and full-hydrogenation of alkynes **2a-g**.

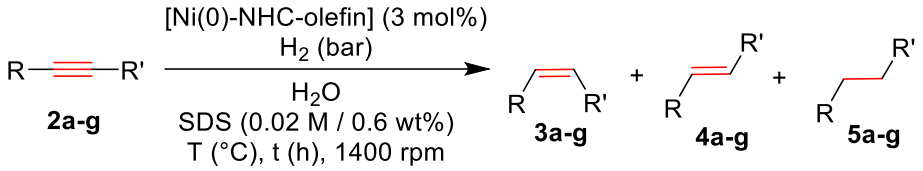

Entry	Alkynes 2 and change of conditions	H_2 (bar)	T (°C)	t (h)	3 +4 yield (%)[a]	4 / 3 (*E* / *Z*) selectivity[a]	5 yield (%)[a]
1	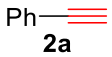 **2a**	1	80	62	0	-	0
2		10	35	13	0	-	Quant.[b]
3	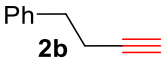 **2b**	10	35	13	-	-	Quant.
4	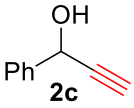 **2c**	10	35	13	-	-	Quant.
5	 **2d**	1	80	62	50	98 / 2	-
6		10	35	13	-	-	Quant.
7	 **2e**	1	80	62	5	97 / 3	-
8		10	35	13	37	-	60
9	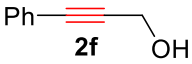 **2f**	1	80	62	98	98 / 2	-
10		10	35	13	13	65 / 35	80
11	**2f, no SDS**	10	35	13	81	20 / 80	19
12	**2f, no SDS, Ni Raney (50 mol%) as catalyst**	10	35	13	-	-	Quant.
13	 **2g**	1	80	62	99	100 / 0	-
14		10	35	13	100	100 / 0	-

[a]Yields and selectivities measured by GC and ^{1}H NMR. Average of at least 2 runs on a 0.5 mmol scale.
[b] Using Brij35 as surfactant; no reaction with SDS

After a first catalytic hydrogenation of phenylpropyne **2d** into phenylpropane **5d** (Table 1, entry 6), macro-rheology measurements were performed on the final reaction solution containing the spent [Ni-NHC-olefin] NPs catalyst. A Newtonian behavior was observed with an almost independent variation of the viscosity as a function of the shear rate with a constant viscosity value close to that of pure water which was very similar to the starting solution containing the fresh catalyst, SDS surfactant and phenylpropyne **2d** (Figures S14 and 3b). Therefore, the morphology of the micelles remained unchanged after a catalysis. In addition, as already highlighted in the discussion related to the catalyst characterization, XPS analysis of a spent catalyst suggested its complete reduction to Ni(0) during the hydrogenation (Figure 1c).

Hydrogenation of Alkenes

The hydrogenation of alkenes catalyzed by Ni-NHC-olefin NPs in SDS-based micelles was also investigated. Terminal alkenes **4a,b** and **4i** were hydrogenated to the corresponding alkanes in high to quantitative yields after 13 h of reaction at 30 °C under 10 bar H_2 (Table 2, entries 1-3). Under similar conditions, the internal alkenes **4d,e** required 24 h of reaction to afford the alkanes **5d,e** in good yields (entries 4,5). By comparison, the hydrogenation of cyano substituted alkene **4j** required a stronger heating to 80 °C and a longer reaction time of 62 h in order to afford quantitatively the alkane **5j** (entry 6) as catalyzed hydrogenations of conjugated nitriles are known to be challenging.[61-63] Similarly, the full hydrogenation of the substituted cyclic alkene, 1-phenylcyclohexene **4l**, to alkane **5l** required a stronger heating to 80 °C in comparison to the reduction of cyclohexene **4k** into **5k** (entries 7,8).[64] It was worth noting that the catalytic hydrogenation of **4l** did not proceed well in pure water, i.e. without the use of SDS, at 10 bar H_2 for 13 h of reaction at 80 °C (entry 9). Furthermore, within similar conditions, the use of Raney Ni as the catalyst in pure water resulted in the quantitative hydrogenation of **4l** into alkane **5l**

(entry 10). Therefore, our catalytic system was rather active and chemoselective but slower than previous studied Pd catalysts stabilized by surfactants. Indeed, by operating under 1 to 14 bar H_2 pressures[15,27-31] or through hydrogen transfer,[19,20,27] they reduced quantitatively alkenes within 0.5 to 12 h, at room temperature or higher in some cases.

Table 2. Catalytic hydrogenation of alkenes **4**.

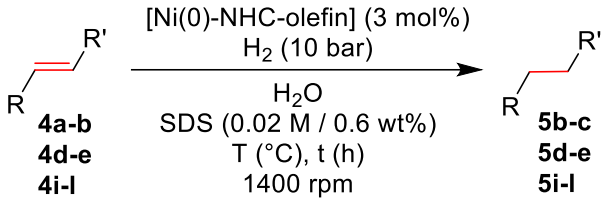

Entry	Alkenes and change of conditions	T (°C)	t (h)	5a-b,5d-e,5i-l Yield (%)[a]
1	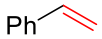 **4a**	30	13	Quant.
2	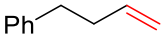 **4b**	30	13	97
3	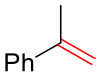 **4i**	30	13	99
4	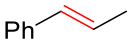 **4d**	30	24	86
5	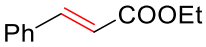 **4e**	30	24	82
6	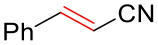 **4j**	80	62	Quant.
7	 **4k**	30	13	93
8	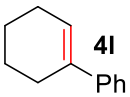 **4l**	80	13	92
9	**4l, no SDS**	80	13	5
10	**4l, no SDS, Ni Raney (50 mol%) as catalyst**	80	13	Quant.

[a] Yields measured by GC. Average of at least 2 runs on a 0.5 mmol scale.

Hydrogenation of Nitroarenes

The Ni-NHC-olefin NPs in SDS-based micelles catalyzed the hydrogenation of nitroarenes to the corresponding anilines in high yields (Table 3) under rather mild conditions, i.e. 10 bar H_2 and 80 °C, by comparison to other nickel catalysts.[65] If nitrobenzene **6a** was quantitatively hydrogenated to aniline in 13 h at 30 °C (entry 1), the *ortho*-fluorinated and *ortho*- and *meta*- methylated nitroarenes **6b-d** required a temperature of 80 °C for the same reaction time to be reduced in good to high yields (entries 2-6). Regarding substrate **6c**, the catalytic hydrogenation proceeded quantitatively in pure water at 10 bar H_2 for 13 h of reaction at 80 °C (entry 5) and, within similar conditions, the use of Raney Ni as catalyst led also to **7c** (entry 6). By comparison, the sterically hindered nitroarenes **6e,f**, functionalized in *ortho* and *ortho'* positions by methyl or fluorine substituents required longer reaction times of 48 and 62 h to be hydrogenated to the corresponding anilines **7e,f** in good yields (entries 5,6). Nevertheless, similar to substrates **6b-d**, the hydrogenation of 4-chloro-3-trifluoromethane-nitrobenzene **6g** proceeded smoothly in 13 h at 80 °C to give aniline **7g** in high yield without any dechlorination (entry 7). Finally, still within these reaction conditions, the alkyne-substituted nitroarene **6h** was reduced quantitatively into aniline **7h** with both alkyne and nitro functions being reduced (entry 8). It was worth to note that the competitive catalytic hydrogenations of nitroarene **6a** and alkene **4b** resulted in trace amounts of aniline **7a** and a low yield of alkane **5b** after 5 h of reaction, the apolar alkene substrate being more reactive than its polar counterpart thanks to stronger interactions with the micelles (Scheme S1). In spite of its chemoselectivity toward chloroarenes, our catalytic system was rather slow by comparison to previous studies on Pd catalysts stabilized by surfactants. Operating under similar H_2 pressure[26,27,32] or through hydrogen transfer,[19,20,23,24] they readily offered reduced nitroarenes within 0.5 to 7 h, at room temperature for some cases.

Table 3. Catalytic hydrogenation of nitroarenes **6** into anilines **7**.

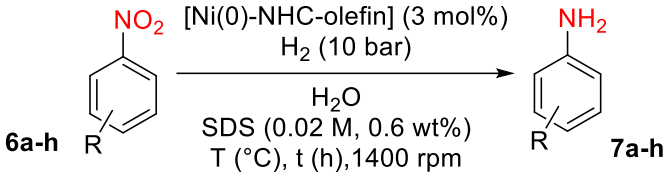

Entry	Nitroarenes 6 and change of conditions	T (°C)	t (h)	Anilines 7a-h yield (%) [1]
1	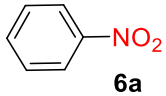 **6a**	30	13	Quant.
2	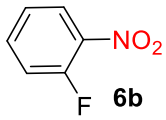 **6b**	80	13	72
3	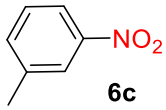 **6c**	80	13	95
4	**6c, no SDS**	80	13	Quant.
5	**6c, no SDS, Ni Raney (50 mol%) as catalyst**	80	13	Quant.
6	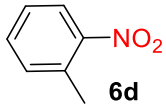 **6d**	80	13	Quant.
7	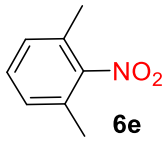 **6e**	80	62	97
8	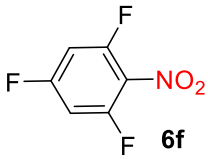 **6f**	80	48	87
9	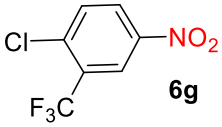 **6g**	80	13	94
10	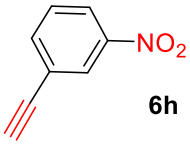 **6h**	80	13	Quant.

[1] Yields measured by GC. Average of at least 2 runs on a 0.5 mmol scale.

Reductive Amination of Aldehydes with Primary Amines

The Ni-NHC-olefin NPs in SDS-based micelles were also active for the reductive amination of aldehydes with primary amines allowing the formation of a broad scope of secondary amines (Scheme 3). The reactions operated in a two step-one-pot procedure starting by the synthesis of imines within the metallomicelles at 80 °C under argon, followed by the hydrogenation under a pressure of 10 bar of H_2, also at 80 °C. At first, benzaldehyde **8a** was reacted with a series of primary amines. While the reactions with aniline **9a** and benzylamine **9c** led to the secondary amines **10aa** and **10ac** in almost quantitative yields within 50 h, the synthesis of the amines **10ab**, **10ad** and **10ae** using mesitylamine **9b**, cyclohexylamine **9d** and furan-2-ylmethanamine **9e** respectively, required 60 h to obtain high yields. Furthermore, by using aniline **9a**, amines **10ba** and **10ca** were prepared in good yields through reaction with aldehydes **8b** and **8c** comprising furan and 2-pyridyl heterocycles. The reactions of substituted benzaldehydes **8d-f** with aniline **9a** afforded the corresponding amines **10da, 10ea** and **10fa** in good to excellent yields, with the presence of an electron-withdrawing substituent such as chloride resulted in a decrease in yield. Finally, the reaction of saturated aldehydes 3-phenylpropanal **8g** and cyclohexylcarboxaldehyde **8h** with benzylamine **9c** or aniline **9a** led to secondary amines **10gc** and **10ha** in good yields. Regarding the reactivity of aldehydes with secondary amines, although we could observe the formation of the imine resulting from the condensation of benzaldehyde and *N*-methyl benzylamine, the catalytic hydrogenation did not proceed. By comparison to other nickel catalysts,[66,67] our catalytic system operated under mild conditions, e.g. temperature and pressure, but required rather long reaction times to achieve good to high yields. Similarly, a previous study on Pd NPs stabilized by a zwitterionic surfactant bearing a sulfonate moiety reported much higher catalytic performances for the reductive amination of benzaldehydes with

primary and secondary amines through transfer hydrogenation and using formate salts as hydrogen donors in aqueous isopropanol,[68] Reactions were performed at 60 - 70 °C and completed in 6 h with TON up to 4900. To complete our study, the developed reaction conditions were applied to the reductive amination of ketones with primary amines studying the reaction of acetophenone **8i** with benzylamine **9c** (Table S4). However, no reactivity was observed even with the use of Brønsted acid additives like acetic acid or dodecylbenzenesulfonic acid.

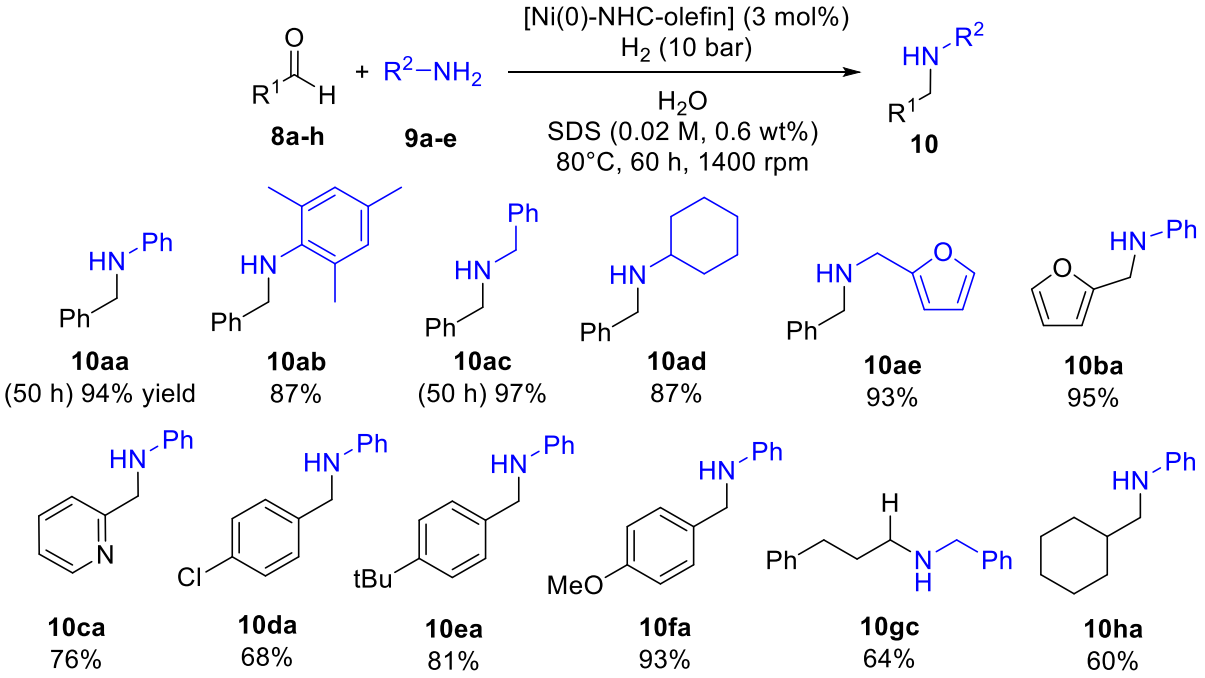

Scheme 3. Reductive amination of aldehydes **8** with primary amines **9**. (yields measured by ^{1}H NMR; average of at least 2 runs on a 0.5 mmol scale).

Catalysis Scale-Up and Catalyst Recycling

The catalytic hydrogenation of phenylacetylene **2a** was scaled-up from 0.5 to 6 mmol (i.e. 0.6 g) of substrate (Table 4). The catalysis afforded a quantitative yield of ethylbenzene **5a** switching from 0.5 to 2 mmol of alkyne (entries 1 and 2). However, such a trend was not applicable to a 4 mmol scale of **2a,** styrene **4a** being the major reaction product (entry 3). This limitation was overcome by a combined increase of the H_2 pressure to 15 bar and of the stirring speed to 2200 rpm, which led to ethylbenzene **5a** in high yield (entry 4). Within these reaction conditions, a kinetic analysis highlighted that an induction period of about 2 h was required before the catalytic hydrogenation started (Figure 5). Such timing likely correlates with a complete reduction and therefore activation of the catalytic species, i.e. Ni-NHC-olefin NPs in SDS micelles, as evidenced by the XPS analysis of the spent catalyst at the end of this scale-up study (Figure 1). Interestingly, by using again a 2200 rpm stirring rate, we were able to effectively perform a 4 mmol scale reaction using twice as little surfactant and water under 10 bar of H_2 (entry 5). In the same trend, the reaction starting from 6 mmol of **2a** proceeded also with less surfactant and water than through their linear increase, but a complete hydrogenation to **5a** required an extended reaction time of 23 h along with 15 bar of hydrogen and a stirring speed of 2200 rpm (entry 6). E factors[69] and PMI[70] were calculated on the best achievements of the scale-up study in order to evaluate the green credentials of the developed synthetic methodology (Table 6 with Table 5, entries 5 and 6). As expected, the calculated data were highly dependent on the selected purification method: interesting low values close from Pd micellar catalysts[31] were obtained when distillation was applied but the extractions led to much higher metrics. The high E factors based on the water used for the reactions highlighted the need for a more effective catalytic process able to operate at higher reagent concentrations.

Table 4. Scale-up of the catalytic full-hydrogenation of alkyne **2a** into alkane **5a**.

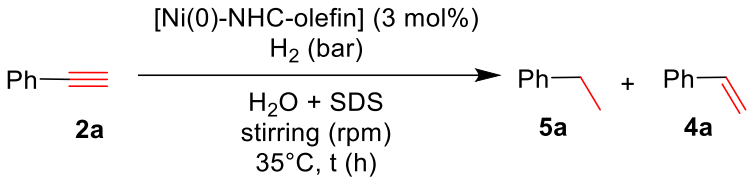

Entry	Alkyne 2a (mmol)	Cat. (mmol)	SDS (mmol)	Volume (mL)	P (bar)	Stirring (rpm)	t (h)	Alkane 5a[a] yield (%)	Alkene 4a[a] yield (%)
1	0.5	0.015	0.1	5	10	1400	13	100	-
2	2	0.06	0.4	20	10	1400	13	100	-
3	4	0.12	0.8	40	10	1400	13	40	60
4	4	0.12	0.8	40	15	2200	13	100 (86)	-
5	4	0.12	0.4	20	10	2200	13	100 (72)	-
6	6	0.18	0.8	40	15	2200	23	100 (88)	-

a. Yields measured by GC; isolated yields in parentheses by extraction and distillation.

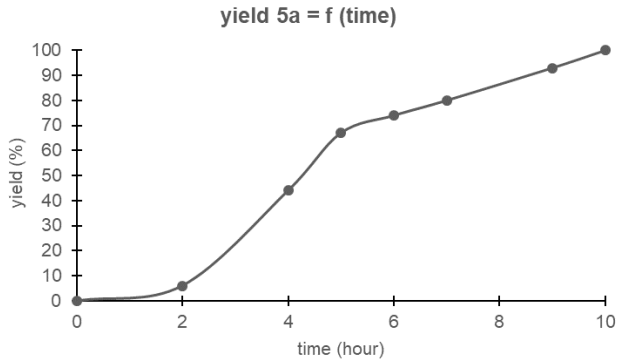

Figure 5. Kinetic profile for the catalytic hydrogenation of alkyne **2a** into alkane **5a** within conditions described in Table 4, entry 4.

Table 5. PMI and E factor for the scale-up of the catalytic full-hydrogenation of alkyne **2a** into alkane **5a** as described in entries 5 and 6 of Table 4.

Catalytic reaction	PMI_{dist}[b] ($g.g^{-1}$)	E $Factor_{dist}$[b] solvent ($g.g^{-1}$)	PMI_{ext}[c] ($g.g^{-1}$)	E $Factor_{ext}$[c] solvent ($g.g^{-1}$)	E Factor water ($g.g^{-1}$)[d]
Table 4, entry 5	4.4[e]	2.8[e]	27.4	25.9	65.4
Table 4, entry 6	2.8[e]	1.5[e]	28.0	26.7	35.7

a. Yields measured by GC; isolated yields in parentheses. b. PMI_{dist} and E $Factor_{dist}$ correspond to the isolation of alkane **5a** by distillation. c. PMI_{ext} and E $Factor_{ext}$ correspond to the isolation of alkane **5a** through extraction with Et_2O. d. Weight of waste water/weight of product. e. Values taking into consideration the use of toluene for the catalyst synthesis.

The catalyst recycling was studied by focusing on the hydrogenation of 4-phenyl-1-butyne **2b** to 1-phenylbutane **5b** at a 0.5 mmol scale (Table 6, Figure S14). The hydrogenations proceeded smoothly over 10 runs with the same catalyst which was separated after each cycle from the organic product through extraction and centrifugation in air. The success of the next catalytic reaction / cycle depended on removing cautiously all CH_2Cl_2 or Et_2O traces under a moderate vacuum and on keeping the same concentration of the catalytic solution (Figure S14). In our hands, the use of a green solvent like EtOAc prevented any recycling likely due its higher boiling point. For 13 h of reaction, the catalytic activity remained remarkably stable along the cycles, as a decrease of yield of only 2% was noticed between the first and 10th runs. However, while focusing on the first hours of the reactions, a regular decrease of TON and TOF was noticed from runs 1 to 7 likely due to the open-air recycling procedure which may lead to a gradual superficial oxidation, or passivation phenomenon. of the Ni catalyst as a function of cycling tests. Nevertheless, the fact that the catalyst was still active at run 8 after 2 h of reaction demonstrates that a reduction period takes place at the beginning of each catalytic run similar to our observations during our kinetic study (Figures 4 and 5). In addition, ICP-AES analyses of the organic phases only evidenced a noticeable leaching of nickel in runs 1 and 2 with respectively 5.4 and 0.3 ppm. Starting from run 3, the Ni leaching remained below 0.08 ppm until run 10. It was worth to note that, after run 1, the isolated organic product **5b** exhibited a minor Ni content of 0.037 (± 0.007) ppm after flash chromatography on 12 g of silica (Table 6). Furthermore, after the first run, a recovery of the leached nickel catalyst was possible through the evaporation of organic solvent and further addition of SDS surfactant (0.6 wt% with respect to the new organic reagent) and water. The resulting new batch of metallomicelles allowed an effective and full catalytic hydrogenation of 4-phenyl-1-butyne **2b** with a 95% yield for alkane **5b** (Scheme 4).

Table 6. Catalyst recycling for the hydrogenation of alkyne **2b** into alkane **5b**

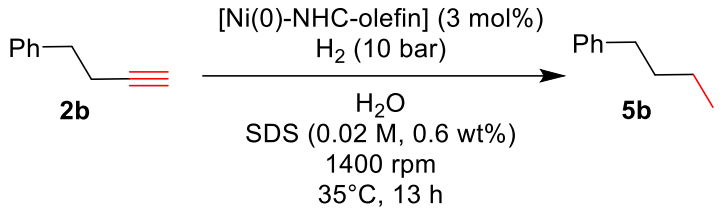

Run	Cycle	Time (h)	Yield[a] 4b (%)	Yield[a] 5b (%)	TON[b]	TOF[c]	Ni leaching[d] (ppm)
1	0	4	55	24	26	7	-
1	0	13	-	Quant.	-	-	5.4[e]
2	1	2	59	13	24	12	-
2	1	13	-	Quant.	-	-	0.3
3	2	2	71	28	33	17	-
3	2	13	-	Quant.	-	-	< 0.08
4	3	1	56	20	25	25	-
4	3	13	-	99	-	-	-
5	4	1	40	19	20	20	-
5	4	13	-	99	-	-	-
6	5	1	29	9	13	13	-
6	5	13	-	99	-	-	< 0.03
7	6	1	13	4	6	6	-
7	6	13	-	99	-	-	-
8	7	2	38	61	33	17	-
8	7	13	-	97	-	-	-
9	8	13	-	98	-	-	-
10	9	13	-	98	-	-	< 0.08[f]

a. Yields measured by GC; 0.5 mmol scale. b. Turnover number = mol of product/mol of catalyst. c. Turnover frequency = mol of product/mol of catalyst/hour. d. Ni leaching in organic phase by ICP-AES. e. 0.037 (± 0.007) ppm of Ni after flash chromatography on 12 g of silica. f. 10.4 ppm of Ni in the aqueous phase.

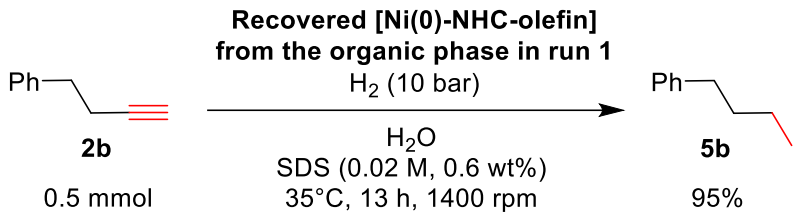

Scheme 4. Recycling of leached Ni in the organic phase.

CONCLUSION

In summary, we report that the combination of NHC-olefin-coordinated Ni nanoparticles with SDS surfactant in water leads to metallomicelles. Such self-assembled structures are effective and reusable catalysts for hydrogenations in water of alkenes, alkynes and nitroarenes as well as for reductive aminations of aldehydes with primary amines. The hydrogenations were scaled up to 6 mmol substrate and the catalyst was recycled over 10 runs without any significant change of activity. By comparison to other nanoparticle-based catalysts confined in micelles, our catalytic system displays interesting features as it allows working with hydrogen gas, in water, without any organic cosolvent and can be recycled. Moreover, the minor amounts of leached Ni catalyst recovered in the organic phase can be recycled as well. However, by comparison to state-of-the-art nanocatalysts based on Pd working under micellar conditions,[5,6] our Ni metallomicelles require improvements as higher loadings, longer times and stronger reaction conditions are required to achieve good to high catalytic activities. Therefore, in order to develop more effective catalytic processes, further developments of such NHC-Ni nanocatalysts are foreseen through appropriate ligand tuning and the use of other confinement strategies.

ASSOCIATED CONTENT

Supporting Information.

The Supporting Information is available free of charge on the ACS Publications website at https://pubs.acs.org/doi/10.1021/acssuschemeng.4c01636

List of items: General methods and instrumentation; additional experimental and analytical data; synthesis, characterization of complex 1; experimental procedures for the catalytic hydrogenations; Characterizations of hydrogenated products; and NMR spectra of complex 1 and all isolated hydrogenated products(PDF)

AUTHOR INFORMATION

Corresponding Author

* Email: cmichon@unistra.fr

ORCID

Marta G. Avello: 0000-0002-3289-020X

Jorge Blas Martínez: 0009-0006-8943-1035

Michael Chetcuti: 0000-0003-0221-7927

Vincent Ritleng: 0000-0002-8480-1491

Cuong Pham-Huu: 0000-0003-3271-019X

Christophe Michon: 0000-0002-0138-2923

Author Contributions

The manuscript was written through contributions of all authors. All authors have given approval to the final version of the manuscript.

Funding Sources

This work has benefitted from the support provided by the University of Strasbourg Institute for Advanced Study (USIAS) for Fellowships, within the French national program "Investment for the future" (IdEx-Unistra) (C.M. and C.P.-H. as fellows, M.G.A. for postdoc). The Cluster of Molecular Chemistry (ClusMolChem) of the European Campus of the Upper Rhine region (EUCOR) is thanked for a grant (C.M. and C.O. as PI and J.B.M. for a Master fellowship). CNRS is warmly acknowledged for its continuous support.

Notes

The authors declare no competing financial interest.

ACKNOWLEDGMENT

This work used the Integrated Structural Biology platform of the Strasbourg Instruct-ERIC center IGBMC-CBI supported by FRISBI (ANR-10-INBS-0005-001) for the Cryo-TEM analysis performed by Dr A. Durand and Dr N. Marechal who are acknowledged for their support. The authors thank Dr. E. Wasielewski and Mr. M. Chessé responsible for the research platforms and facilities (Strasbourg NMR plateform and Strasbourg chromatography facilities) of LIMA (UMR7042 CNRS-Unistra-UHA) who contributed, by their valuable technical and scientific support, to the achievement of this research project. Dr J.-M. Strub (IPHC UMR7178 CNRS-Unistra) is acknowledged for the HRMS analyses. Dr A. Boos, Mrs P. Ronot and Mrs I. El Masoudi (IPHC UMR7178 CNRS-Unistra) are acknowledged for the ICP-AES analyses. Mr S. Sall (ICPEES UMR7113 CNRS-Unistra) is acknowledged for his assistance with ATG analyses. Dr J.-F. Nierengarten (LIMA UMR7042 CNRS-Unistra-UHA) is acknowledged for granting us an unlimited access to his centrifuge.

ABBREVIATIONS

Binding Energy (BE); Polyethyleneglycol lauryl ether (Brij® 35); transmission electron cryomicroscopy (CryoTEM); gas chromatography (GC); inductively coupled plasma – atomic emission spectroscopy (ICP-AES); Multiple Particle Tracking (MPT); N-heterocyclic carbene (NHC); nuclear magnetic resonance (NMR); Metal nanoparticles (NPs); process mass intensity (PMI); round per minute (RPM); sodium dodecyl sulfate (SDS); Scanning Electron Microscopy - Scanning Transmission Electron Microscopy (SEM-STEM); tetrahydrofuran (THF); X-ray photoelectron spectroscopy (XPS).

REFERENCES

(1) Terra, J. C. S.; Martins, A. R.; Moura, F. C. C.; Weber, C. C.; Moores, A. Making more with less: confinement effects for more sustainable chemical transformations. *Green Chem.* **2022**, *24*, 1404–1438. DOI: 10.1039/d1gc03283f

(2) Andersson, M. P. Entropy reduction from strong localization – an explanation for enhanced reaction rates of organic synthesis in aqueous micelles. *J. Colloid Interface Sci.* **2022**, *628*, 819–828. DOI: 10.1016/j.jcis.2022.08.105

(3) Cortes-Clerget, M.; Yu, J.; Kincaid, J. R. A.; Walde, P.; Gallou, F.; Lipshutz, B. H. Water as the reaction medium in organic chemistry: from our worst enemy to our best friend, *Chem. Sci.* **2021**, *12*, 4237-4266. DOI: 10.1039/D0SC06000C

(4) Heddouin, G.; Ogulu, D.; Kaur, G.; Handa, S. Aqueous micellar technology: an alternative beyond organic solvents. *Chem. Commun.* **2023**, *59*, 2842-2853. DOI: 10.1039/D3CC00127J

(5) Wu, B.; Miraghaee, S.; Handa, S.; Gallou, F. Nanoparticles for catalysis in aqueous media. *Curr. Opin. Green Sustain. Chem.* **2022**, *38*, 100691. DOI: 10.1016/j.cogsc.2022.100691

(6) Thakore, R. R.; Iyer, K. S.; Lipshutz, B. H.; Sustainable routes to amines in recyclable water using ppm Pd catalysis. *Curr. Opin. Green Sustain. Chem.* **2021**, *31*, 100493. DOI: 10.1016/j.cogsc.2021.100493

(7) Scarso, A.; Strukul, G. Transition Metal Catalysis in Micellar Media: Much More Than a Simple Green Chemistry Promise. In *Green Chemistry Series No. 61 Green Synthetic Processes and Procedures;* Ballini, R. Ed; Royal Society of Chemistry, **2019**; chapter 12*,* pages 268–288.

(8) Fabris, F.; Illner, M.; Repke, J. U.; Scarso, A.; Schwarze, M. Is Micellar Catalysis Green Chemistry? *Molecules* **2023**, *28*, 4809. DOI: 10.3390/molecules28124809

(9) Nagarajan, R. Self-Assembly from Surfactants to Nanoparticles – Head vs. Tail, In: Self-Assembly: From Surfactants to Nanoparticles, Nagarajan, R. E. John Wiley & Sons, Inc. December 2018; chapter 1, pages 1-40. DOI: 10.1002/9781119001379

(10) Wei, W.; Bai, F.; Fan, H. Surfactant-Assisted Cooperative Self-Assembly of Nanoparticles into Active Nanostructures. *iScience* **2019**, *11*, 272–293. DOI: 10.1016/j.isci.2018.12.025

(11) Nikoobakht, B.; El-Sayed, M. A. Evidence for Bilayer Assembly of Cationic Surfactants on the Surface of Gold Nanorods. *Langmuir* **2001**, *17*, 6368-6374. DOI: 10.1021/la010530o

(12) Fu, L.; Dravid, V. P.; Johnson, D. L. Self-Assembled (SA) bilayer molecular coating on magnetic nanoparticles. *Appl. Surf. Sci.* **2001**, *181*, 173-178. DOI: 10.1016/S0169-4332(01)00388-9

(13) Wu, S.-H.; Chen, D.-H. Synthesis of high-concentration Cu nanoparticles in aqueous CTAB solutions. *J. Colloid Interface Sci.* **2004**, *273*, 165–169. DOI: 10.1016/j.jcis.2004.01.071

(14) Guyonnet Bilé, E.; Sassine, R.; Denicourt-Nowicki, A.; Launay, F.; Roucoux, A. New ammonium surfactant-stabilized rhodium(0) colloidal suspensions: Influence of novel counter-anions on physico-chemical and catalytic properties. *Dalton Trans.* **2011**, *40*, 6524–6531. DOI: 10.1039/c0dt01763a

(15) Souza, B. S.; Leopoldino, E. C.; Tondo, D. W.; Dupont, J.; Nome, F. Imidazolium-Based Zwitterionic Surfactant: A New Amphiphilic Pd Nanoparticle Stabilizing Agent. *Langmuir* **2012**, *28*, 833–840. DOI: 10.1021/la203501f

(16) Handa, S.; Wang Y.; Gallou F.; Lipshutz, B. H. Sustainable Fe-ppm Pd nanoparticle catalysis of Suzuki-Miyaura cross-couplings in water. *Science* **2015**, *349*,1087–1091. DOI: 10.1126/science.aac6936

(17) Wood, A. B.; Nandiwale K. Y.; Mo, Y.; Jin, B.; Pomberger, A.; Schultz, V. L.; Gallou, F.; Jensen, K. F., Lipshutz, B. H: Continuous flow Suzuki-Miyaura couplings under aqueous micellar conditions in a CSTR cascade catalyzed by Fe/ppm Pd nanoparticles. *Green Chem.* **2020**, *22*, 3441–3444. DOI: 10.1039/D0GC00378F

(18) Pang, H.; Hu, Y.; Yu, T.; Gallou, F.; Lipshutz, B. H. Water-sculpting of a heterogeneous nanoparticle pre-catalyst for Mizoroki-Heck couplings under aqueous micellar catalysis conditions. *J. Am. Chem. Soc.* **2021**, *143*, 3373–3382. DOI: 10.1021/jacs.0c11484

(19) Oba, M.; Kojima, K.; Endo, M.; Sano, H.; Nishiyama, K. Palladium-catalyzed transfer hydrogenation of organic substrates by hypophosphite in water containing a nonionic surfactant. *Green Chem. Lett. Rev.* **2013**, *6*, 233-236, DOI: 10.1080/17518253.2012.754498

(20) Batarseh, C.; Nairoukh, Z.; Volovych, I.; Schwarze, M.; Schomäcker, R.; Fanun, M.; Blum, J. Catalytic transfer hydrogenation of hydrophobic substrates by water-insoluble hydrogen donors in aqueous microemulsions. *J. Mol. Catal. A: Chem.* **2013**, *366*, 210–214. DOI: 10.1016/j.molcata.2012.09.025

(21) Slack, E. D.; Gabriel, C. M.; Lipshutz, B. H. A Palladium Nanoparticle–Nanomicelle Combination for the Stereoselective Semihydrogenation of Alkynes in Water at Room Temperature. *Angew. Chem. Int. Ed.* **2014**, *53*, 14051–14054. DOI: 10.1002/anie.201407723

(22) La Sorella, G.; Canton, P.; Strukul, G.; Scarso, A. Surfactant-Induced Substrate Selectivity in the Palladium-Nanoparticle-Mediated Chemoselective Hydrogenation of Unsaturated Aldehydes in Water. *ChemCatChem* **2014**, *6*, 1575–1578. DOI: 10.1002/cctc.201402034

(23) Souza, F. D.; Fiedler, H.; Nome, F. Zwitterionic Surfactant Stabilized Palladium Nanoparticles as Catalysts in Aromatic Nitro Compound Reductions. *J. Braz. Chem. Soc.* **2015**, *27*, 372-381. DOI: 10.5935/0103-5053.20150284

(24) Gabriel, C. M.; Parmentier, M.; Riegert, C.; Lanz, M.; Handa, S.; Lipshutz, B. H.; Gallou, F. Sustainable and Scalable Fe/ppm Pd Nanoparticle Nitro Group Reductions in Water at Room Temperature. *Org. Process Res. Dev.* **2017**, *21*, 247−252. DOI: 10.1021/acs.oprd.6b00410

(25) La Sorella, G.; Sperni, L.; Canton, P.; Coletti, L.; Fabris, F.; Strukul, G.; Scarso, A. Selective Hydrogenations and Dechlorinations in Water Mediated by Anionic Surfactant-Stabilized Pd Nanoparticles. *J. Org. Chem.* **2018**, *83*, 7438−7446. DOI: 10.1021/acs.joc.8b00314

(26) Liang, C.; Han, J.; Shen, K.; Wang, L.; Defeng Zhao, D.; Freeman, H. S. Palladium nanoparticle microemulsions: Formation and use in catalytic hydrogenation of o-chloronitrobenzene. *Chem. Eng. J.* **2010**, *165*, 709–713. DOI: 10.1016/j.cej.2010.10.022

(27) Zhu, W.; Yang, H.; Yu, Y.; Hua, L.; Li, H.; Feng, B.; Hou, Z. Amphiphilic ionic liquid stabilizing palladium nanoparticles for highly efficient catalytic hydrogenation. *Phys. Chem. Chem. Phys.* **2011**, *13*, 13492–13500. DOI: 10.1039/c1cp20255c

(28) Weiss, E.; Dutta, B.; Schnell, Y.; Abu-Reziq, R. Palladium nanoparticles encapsulated in magnetically separable polymeric nanoreactors. *J. Mater. Chem. A* **2014**, *2*, 3971–3977. DOI: 10.1039/C3TA14992G

(29) Arbelaez, O.; Correa, L.; Parapat, R. Y.; Knemeyer, K.; Bustamante, F.; Luz Villa, A.; Schwarze, M. Pd@Al_2O_3-Catalyzed Hydrogenation of Allylbenzene to Propylbenzene in Methanol and Aqueous Micellar Solutions. *Chem. Eng. Technol.* **2015**, *38*, 2291–2298. DOI: 10.1002/ceat.201500316

(30) Albuquerque, B. L.; Denicourt-Nowicki, A.; Mériadec, C.; Josiel B. Domingos, J. B.; Roucoux, A. Water soluble polymer–surfactant complexes-stabilized Pd(0) nanocatalysts: Characterization and structure–activity relationships in biphasic hydrogenation of alkenes and α,β-unsaturated ketones. *J. Catal.* **2016**, *340*, 144–153. DOI: 10.1016/j.jcat.2016.05.015

(31) Takale, B. S.; Thakore, R. R.; Gao, S. E.; Gallou, F.; Lipshutz, B. H. Environmentally responsible, safe, and chemoselective catalytic hydrogenation of olefins: ppm level Pd catalysis in recyclable water at room temperature. *Green Chem.* **2020**, *22*, 6055–6061. DOI: 10.1039/d0gc02087g

(32) Li, X.; Thakore, R. R.; Takale, B. S.; Gallou, F.; Lipshutz, B. H. High Turnover Pd/C Catalyst for Nitro Group Reductions in Water. One-Pot Sequences and Syntheses of Pharmaceutical Intermediates. *Org. Lett.* **2021**, *23*, 8114−8118. DOI: 10.1021/acs.orglett.1c03258

(33) Luescher, M. U.; Gallou, F.; Lipshutz, B. H. The impact of earth-abundant metals as a replacement for Pd in cross coupling reactions. *Chem. Sci.* **2024**, *15*, 9016 −9025. DOI: 10.1039/D4SC00482E.

(34) Cushing, B. L.; Kolesnichenko, V. L.; O'Connor, C. J. Recent Advances in the Liquid-Phase Syntheses of Inorganic Nanoparticles. *Chem. Rev.* **2004**, *104*, 3893-3946. DOI: 10.1021/cr030027b

(35) Ott; L. S.; Finke, R. G. Transition-metal nanocluster stabilization for catalysis: A critical review of ranking methods and putative stabilizers. *Coord. Chem. Rev.* **2007**, *251*, 1075-1100. DOI: 10.1016/j.ccr.2006.08.016

(36) Heuer-Jungemann, A.; Feliu, N.; Bakaimi, I.; Hamaly, M.; Alkilany, A.; Chakraborty, I.; Masood, A.; Casula, M. F.; Kostopoulou, A.; Oh, E.; Susumu, K.; Stewart, M. H.; Medintz, I. L.; Stratakis, E.; Parak, W. J.; Kanaras, A. G. The role of ligands in the chemical synthesis and applications of inorganic nanoparticles. *Chem. Rev.* **2019**, *119*, 4819-4880. DOI: 10.1021/acs.chemrev.8b00733

(37) Lu, L.; Zou, S.; Fang, B. The Critical Impacts of Ligands on Heterogeneous Nanocatalysis: A Review, *ACS Catal.* **2021**, *11*, 6020-6058. DOI: 10.1021/acscatal.1c00903

(38) Zhukhovitskiy, A. V.; MacLeod, M. J.; Johnson, J. A. Carbene Ligands in Surface Chemistry: From Stabilization of Discrete Elemental Allotropes to Modification of Nanoscale and Bulk Substrates. *Chem. Rev.* **2015**, *115*, 11503-11532. DOI: 10.1021/acs.chemrev.5b00220

(39) Zhong, R.; Lindhorst, A. C.; Groche, F. J.; Kühn, F. E. Immobilization of N-Heterocyclic Carbene Compounds: A Synthetic Perspective. *Chem. Rev.* **2017**, *117*, 1970-2058. DOI: 10.1021/acs.chemrev.6b00631

(40) Ghosh, M.; Khan, S. N-Heterocyclic Carbenes Capped Metal Nanoparticles: An Overview of Their Catalytic Scope. *ACS Catal.* **2023**, *13*, 9313-9325. DOI: 10.1021/acscatal.3c01824

(41) Soulé, J.-F.; Miyamura, H.; Kobayashi, S. Copolymer-Incarcerated Nickel Nanoparticles with N-Heterocyclic Carbene Precursors as Active Cross-Linking Agents for Corriu–Kumada–Tamao Reaction. *J. Am. Chem. Soc.* **2013**, *135*, 10602-10605. DOI: 10.1021/ja404006w

(42) Díaz de Los Bernardos, M.; Pérez-Rodríguez, S.; Gual, A.; Claver, C.; Godard, C. Facile synthesis of NHC-stabilized Ni nanoparticles and their catalytic application in the Z-selective hydrogenation of alkynes. *Chem. Commun.* **2017**, *53*, 7894-7897. DOI: 10.1039/C7CC01779K

(43) Bouzoita, D.; Asensio, J. M.; Pfeifer, V.; Palazzolo, A.; Lecante, P.; Pieters, G.; Feuillastre, S.; Tricard, S.; Chaudret, B. Chemoselective H/D exchange catalyzed by nickel nanoparticles stabilized by N-heterocyclic carbene ligands. *Nanoscale* **2020**, *12*, 15736-15742. DOI: 10.1039/D0NR04384B

(44) Ulm, F.; Shahane, S.; Truong-Phuoc, L.; Romero, T.; Papaefthimiou, V.; Chessé, M.; Chetcuti, M. J.; Pham-Huu, C.; Michon, C.; Ritleng, V. Half-Sandwich Nickel(II) NHC-Picolyl Complexes as Catalysts for the Hydrosilylation of Carbonyl Compounds: Evidence for NHC-Nickel Nanoparticles under Harsh Reaction Conditions. *Eur. J. Inorg. Chem.* **2021**, 3074-3082. DOI: 10.1002/ejic.202100371

(45) Garcia, M.; Golling, S.; Truong-Phuoc, L.; Vidal, L.; Romero, T.; Papaefthimiou, V.; Gruber, N.; Chetcuti, M. J.; Leroux, F. R., Donnard, M.; Ritleng, V.; Pham-Huu, C., Michon, C. (NHC-olefin)-nickel(0) nanoparticles as catalysts for the (*Z*)-selective semi-hydrogenation of alkynes and ynamides. *Chem. Commun.* **2023**, *59*, 1537-1540. DOI: 10.1039/d2cc05302k

(46) Israelachvili, J. N.; Mitchell, D. J.; Ninham, B. W. Theory of self-assembly of hydro-carbon amphiphiles into micelles and bilayers. *J. Chem. Soc. Faraday Trans. 2* **1976**, *72*, 1525-1568. DOI: 10.1039/F29767201525

(47) Yin, H.; Lei, S.; Zhu, S.; Huang, J.; Ye, J. Micelle-to-vesicle transition induced by organic additives in cationic surfactant systems. *Chem. Eur. J.* **2006**, *12*, 2825-2835. DOI: 10.1002/chem.200501053

(48) Wang, J. Z.; Song, A. X.; Jia, X. F.; Hao, J. C.; Liu, W. M.; Hoffmann, H. Two routes to vesicle formation: metal-ligand complexation and ionic interactions, *J. Phys.Chem. B* **2005**, *109*, 11126-11134. DOI: 10.1021/jp044518r

(49) Du, N.; Song, R.; Zhang, H.; Sun, J.; Yuan, S.; Zhang, R.; Hou, W. The formation and stability of sodium dodecylsulfate vesicles mediated by rough glass surface. *Colloids Surf. A* **2016**, *509*, 195-202. DOI: 10.1016/j.colsurfa.2016.09.006

(50) Bergström, M.; Pedersen, J. S. Small-Angle Neutron Scattering (SANS) Study of Aggregates Formed from Aqueous Mixtures of Sodium Dodecyl Sulfate (SDS) and Dodecyltrimethylammonium Bromide (DTAB). *Langmuir* **1998**, *14*, 3754–3761. DOI: 10.1021/la980107o

(51) Andersen, K. K.; Oliveira, C. L.; Larsen, K. L.; Poulsen, F. M.; Callisen, T. H.; Westh, P.; Pedersen, J. S.; Otzen, D. The Role of Decorated SDS Micelles in Sub-CMC Protein Denaturation and Association. *J. Mol. Biol.* **2009**, *391*, 207–226. DOI: 10.1016/j.jmb.2009.06.019

(52) Hammouda, B. Temperature Effect on the Nanostructure of SDS Micelles in Water. *J. Res. NIST* **2013**, *118*, 151–167. DOI: 10.6028/jres.118.008

(53) Ikeda, S.; Ozeki, S.; Hayashi, S. Size and shape of charged micelles of ionic surfactants in aqueous salt solutions. *Biophys. Chem.* **1980**, *11*, 417-423. DOI: 10.1016/0301-4622(80)87016-5

(54) Magid, L. J.; Li, Z.; Butler, P. D. Flexibility of Elongated Sodium Dodecyl Sulfate Micelles in Aqueous Sodium Chloride: A Small-Angle Neutron Scattering Study. *Langmuir* **2000**, *16*, 10028-10036. DOI: 10.1021/la0006216

(55) Jensen, G. V.; Lund, R.; Gummel, J.; Narayanan, T.; Pedersen, J. S. Monitoring the Transition from Spherical to Polymer-like Surfactant Micelles Using Small-Angle X-Ray Scattering. *Angew. Chem. Int. Ed.* **2014**, *53*, 11524-11528. DOI: 10.1002/anie.201406489

(56) Minkler, S. R. K.; Lipshutz, B. H.; Krause, N. Gold Catalysis in Micellar Systems. *Angew. Chem. Int. Ed.* **2011**, *50*, 7820-7823. DOI: 10.1002/anie.201101396

(57) Lempke, L.; Ernst, A.; Kahl, F.; Weberskirch, R.; Krause, N. Sustainable Micellar Gold Catalysis – Poly(2-oxazolines) as Versatile Amphiphiles. *Adv. Synth. Catal.* **2016**, *358*, 1491-1499. DOI: 10.1002/adsc.201600139

(58) Petersen, H.; Ballmann, M.; Krause, N.; Weberskirch, R. Gold(I) NHC Catalysts Immobilized to Amphiphilic Block Copolymers: A Versatile Approach to Micellar Gold Catalysis in Water. *ChemCatChem* **2022**, *14*, e202200727. DOI: 10.1002/cctc.202200727

(59) Ramirez, B. L.; Lu, C. C. Rare-Earth Supported Nickel Catalysts for Alkyne Semihydrogenation: Chemo- and Regioselectivity Impacted by the Lewis Acidity and Size of the Support. *J. Am. Chem. Soc.* **2020**, *142*, 5396−5407. DOI: 10.1021/jacs.0c00905

(60) Hale, D. J.; Ferguson, M. J.; Turculet, L. (PSiP)Ni-Catalyzed (*E*)-Selective Semihydrogenation of Alkynes with Molecular Hydrogen. *ACS Catal.* **2022**, *12*, 146−155. DOI: 10.1021/acscatal.1c04537

(61) Müller, M.-A.; Pfaltz, A. Asymmetric Hydrogenation of α,β-Unsaturated Nitriles with Base-Activated Iridium N,P Ligand Complexes. *Angew. Chem. Int. Ed.* **2014**, *53*, 8668-8671. DOI: 10.1002/anie.201402053

(62) Yan, Q.; Kong, D.; Li, M.; Hou, G., Zi, G. Highly Efficient Rh-Catalyzed Asymmetric Hydrogenation of α,β-Unsaturated Nitriles. *J. Am. Chem. Soc.* **2015**, *137*, 10177-10181. DOI: 10.1021/jacs.5b06418

(63) Kong, D.; Li, M.; Wang, R.; Zi, G.; Hou, G. Asymmetric Hydrogenation of β-Aryloxy/Alkoxy Cinnamic Nitriles and Esters. *Org. Lett.* **2016**, *18*, 4916-4919. DOI: 10.1021/acs.orglett.6b02393

(64) Viereck, P.; Krautwald, S.; Pabst, T. P.; Chirik, P. J. A boron activating effect enables cobalt-catalyzed asymmetric hydrogenation of sterically hindered alkenes. *J. Am. Chem. Soc.* **2020**, *142*, 3923–3930. DOI: 10.1021/jacs.9b12214

(65) Formenti, D.; Ferretti, F.; Scharnagl, F. K.; Beller, M. Reduction of Nitro Compounds Using 3d-Non-Noble Metal Catalysts. *Chem. Rev.* **2019**, *119*, 2611−2680. DOI: 10.1021/acs.chemrev.8b00547.

(66) Irrgang, T.; Kempe, R. Transition-Metal-Catalyzed Reductive Amination Employing Hydrogen. *Chem. Rev.* **2020**, *120*, 9583−9674. DOI: 10.1021/acs.chemrev.0c00248

(67) Liu, J.; Song, Y.; Ma, L. Earth-abundant Metal-catalyzed Reductive Amination: Recent Advances and Prospect for Future Catalysis. *Chem.-Asian J.* **2021**, *16*, 2371–2391. DOI: 10.1002/asia.202100473

(68) Drinkel, E. E.; Campedelli, R. R.; Manfredi, A. M.; Fiedler, H. D.; Nome, F. Zwitterionic-Surfactant-Stabilized Palladium Nanoparticles as Catalysts in the Hydrogen Transfer Reductive Amination of Benzaldehydes. *J. Org. Chem.* **2014**, *79*, 2574−2579. DOI: 10.1021/jo5000362

(69) Sheldon., R. A. The E Factor: fifteen years on. *Green Chem.* **2007**, *9*, 1273–1283. DOI: 10.1039/b713736m

(70) Monteith, E. R.; Mampuys, P.; Summerton, L.; Clark, J. H.; Maes, B. U. W.; McElroy, C. R.; Why we might be misusing process mass intensity (PMI) and a methodology to apply it effectively as a discovery level metric. *Green Chem.* **2020**, *22*, 123–135. DOI: 10.1039/c9gc01537j